DOI: 10.1021/ma901037c

Macromolecules
COMMUNICATION TO THE EDITOR

Regular Network Pattern Evolution Observed in Phase Separation in Low-Molecular-Weight LC and LC Block Copolymer Mixture

Osamu Sato,[†] Yusuke Inagaki,[‡] Sungmin Kang,[‡] Masatoshi Tokita,[‡] and Junji Watanabe*,[‡]

[†]*Japan Laboratory, LG Display Co., Ltd., 453 German Centre, 1-18-2 Hakusan, Midori-ku, Yokohama 226-0006, Japan, and* [‡]*Department of Organic and Polymeric Materials, Tokyo Institute of Technology, O-okayama, Meguro-ku, Tokyo 152-8552, Japan*

Received May 12, 2009
Revised Manuscript Received July 9, 2009

Phase separation phenomena have been widely studied for various materials including liquids and complex fluids such as polymers, colloids, liquid crystals, and biological materials,[1−3] and pattern evolution of immiscible component mixtures has been discussed with parameters characteristic of materials and/or material states. In liquid-crystalline (LC) systems, phase separation will proceed through a competition between interfacial surface energy and elastic distortion energy, which is expected to show characteristic pattern evolution. For this reason, many studies on phase separation have been reported by treating flexible polymer/LC mixture systems.[4] However, there are only a few reports on LC polymer/LC mixture.[5,6] In this study, we examined phase separation behavior in binary nematic mixtures of LC block copolymer (LC-BP) and low-molecular-weight LC material (LMW-LCM) in a homogeneously aligned thin cell. During the phase separation, excellent pattern evolution was observed such that the LMW-LCM-rich nematic phase is accommodated in the microcell divided by a honeycomb network wall of the LC-BP-rich nematic phase.

LMW-LCM (commercially named JC-5066**) was used as supplied by Chisso Co., Ltd. Nematic LC in LMW-LCM is stably formed at room temperature and has an isotropization temperature of 72 °C. LC-BP used in this study is composed of polystyrene and a side-chain LC polymer (so-called PM6ME) with the following chemical structure

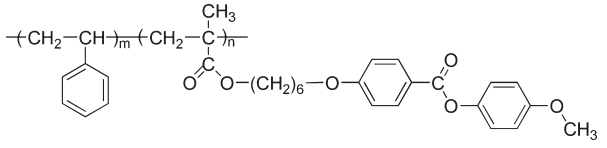

which was obtained by atom transfer radical polymerization.[7,8] The number-averaged molecular weight M_n and the polydispersity M_w/M_n as determined from gel permeation chromatography in chloroform solution on the basis of the calibration of standard polystyrene are 29 500 and 1.37, respectively. The weight fraction of LC PM6ME segment in LC-BP was determined to be 88 wt % by ^{1}H NMR spectra. This copolymer was found to form cylindrical microsegregation structure in which PS microcylinders are dispersed in liquid-crystalline PM6ME matrix.[8] The PM6ME matrix forms smectic A (S_A), nematic (N), and isotropic liquid (Iso) phases in order of increasing temperature. No crystallization takes place; hence, the S_A phase vitrifies on cooling to room temperature. The temperatures of glass−S_A, S_A−N, and N−Iso transitions are 42, 70, and 101 °C, respectively, as determined by differential scanning calorimetry (Perkin-Elmer Pyris1 DSC) at a heating rate of 10 °C min^{-1}.

*Corresponding author. E-mail: jwatanab@polymer.titech.ac.jp.

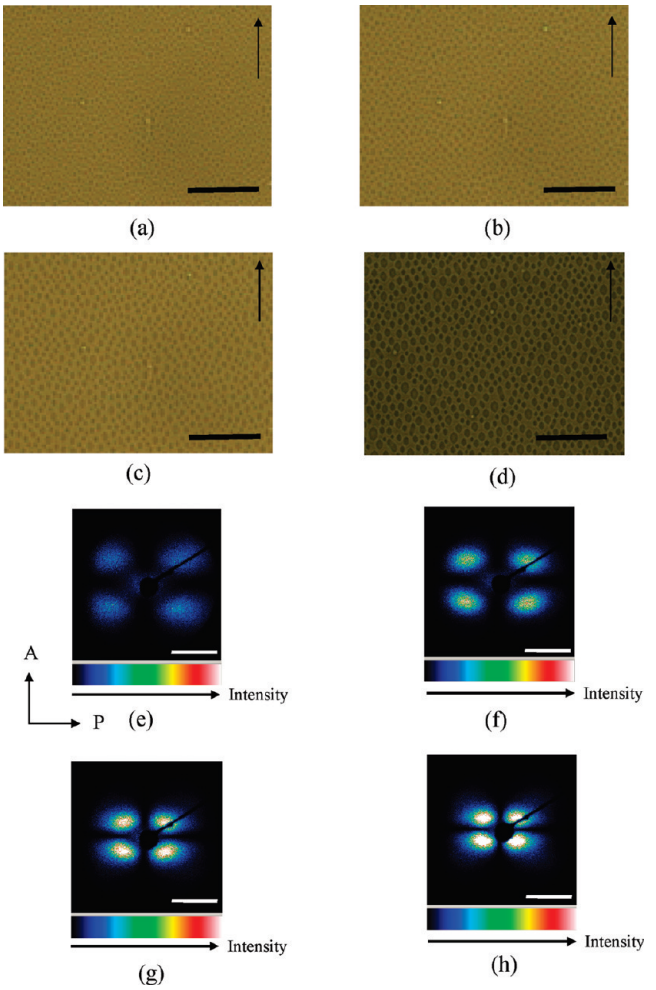

Figure 1. (a−d) Optical micrographs and (e−h) light scattering patterns of mixture with the LC-BP fraction of 25 wt %, observed at 38 °C after (a, e) 5, (b, f) 10, (c, g) 30, and (d, h) 60 min of isothermal phase separation at 38 °C. In (a−d), the scale bar is 50 μm and the arrow indicates the rubbing direction. Light scattering patterns were measured under the *Hv* condition with the polarizer perpendicular to the rubbing direction and are shown in (e−h) in an identical intensity range. The scale bar is $q = 2\,\mu m^{-1}$.

Mixtures of LC-BP and LMW-LCM were prepared by solvent casting from dichloromethane solutions. All the mixtures with LC-BP weight fractions ranged from 0 to 35 wt % form a uniform nematic phase in the higher temperature region, which transforms to the isotropic liquid at 72−75 °C. On cooling, the nematic−nematic phase separation takes place between the LC-BP-rich and LMW-LCM-rich phases, giving an upper critical solution temperature (UCST) type phase diagram (refer to Figure S1 of the Supporting Information). The critical composition and temperature are 6 wt % of the LC-BP weight fraction and 47 °C, respectively.

The phase separation behavior was examined for the homogeneous nematic monodomain sample in a thin cell. The nematic

 Published on Web 07/20/2009 © 2009 American Chemical Society

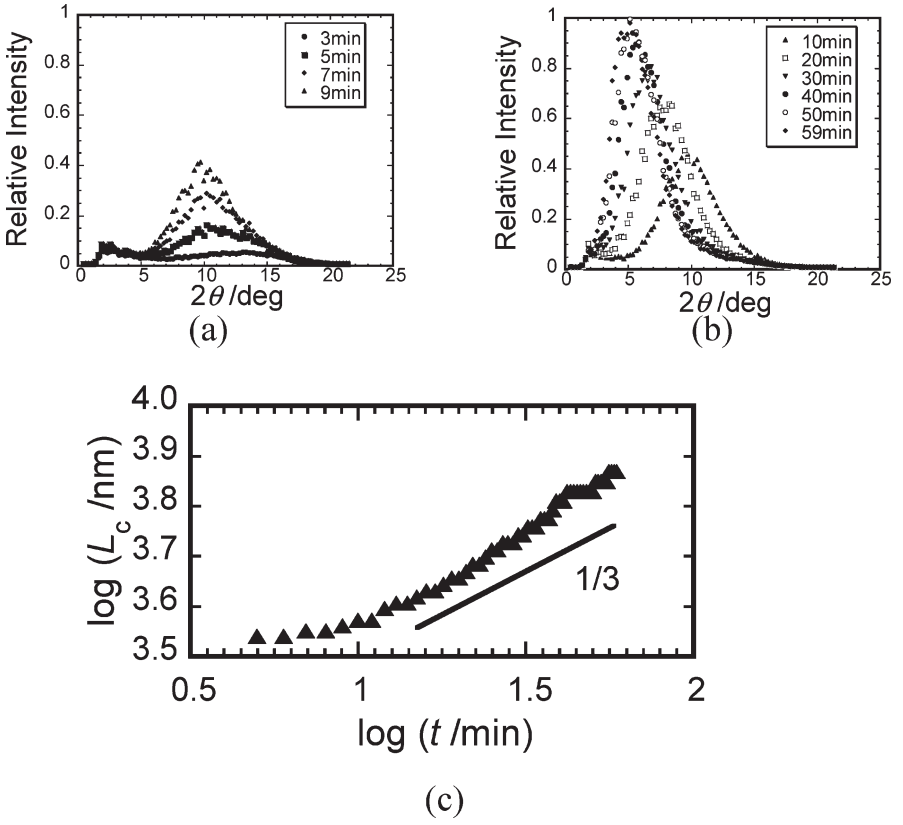

Figure 2. (a, b) Intensity profiles of scattering light in the first and late stages, respectively, and (c) logarithmic plot of the correlation length L_c vs time spent for the isothermal phase separation of mixture with the LC-BP fraction of 25 wt % at 38 °C. As reference, a solid line with a slope of 1/3 is shown.

monodomain was obtained by a conventional method in which the mixture was sandwiched between two polyimide-coated glass plates that were rubbed to promote homogeneous molecular orientation. The cell gap was 3 μm. Within the thin cell, phase separation takes place differently from that in the bulk sample. When the weight fraction of LC-BP is smaller than 15 wt %, the phase separation seems not to take place at any temperature, and the nematic monodomain remains unchanged on cooling to room temperature. As a possible explanation, surface-induced segregation[9] takes place as a result of interfacial interactions with cell walls as has been observed in thin film of polymer blend as well as diblock copolymer confined between two slabs.[10,11] The polymer-rich phase may be preferentially segregated as thin layers on the surfaces of two cell walls so that no apparent phase-separated domain texture is detected in the microscopic observation. In this study, then, phase separation was examined for a mixture with the LC-BP fraction of 25 wt % under the following procedure.

To eliminate the preceding thermal history, initially, the sample was heated up to the isotropic temperature of 80 °C and then cooled to the nematic temperature of 50 °C. After formation of uniform nematic monodomain was ensured, the sample cell was quenched down to 38 °C within a few seconds to induce isothermal nematic−nematic phase separation (refer to Figure S1). From Figure S1, the two phase-separated nematic phases are found to be LMW-LCM-rich nematic phase with a LC-BP fraction of 2 wt % and LC-BP-rich nematic phase with a LC-BP fraction of 32 wt %. Figures 1a−d show microscopic domain evolution observed during phase separation under an Olympus BX50 polarized optical microscope (POM) equipped with a Mettler FP82HT hot stage. First, small droplets of minority LMW-LCM-rich phase are immediately formed (see Figure 1a). This phase separation behavior is typical of droplet spinodal decomposition. The droplets coarsen with time by repeated collisions and coalescence[12−14] and also by an evaporation−condensation process[15] (Figures 1b,d), thereby forming regular arrays of droplets.

Time evolution of the phase separation pattern was also investigated using two-dimensional light scattering patterns, which were measured under the *H*v condition with a CCD camera mounted in an Otsuka Electronics DYNA-3000. Here, the rubbing direction of the cell was set parallel to the analyzer axis direction. Figures 1e−h show light scattering intensity profiles at different isothermal periods. Of interest is that the scattering does not appear as a ring, but at definite azimuthal directions tilting by 60° to the rubbing direction (n-director of nematic phase), which is attributed to the two-dimensionally periodic density fluctuation. The reason for this characteristic scattering direction will be discussed later. In the first stage up to 10 min (Figure 1e), the scattering that may be assigned to the spinodal one increases its intensity without changing the peak position. With increasing time in the late stage, the peak position shifts toward the small-angle region (see Figures 1f−h). The correlation length L_c ($= \lambda/2 \sin \theta$), estimated from the peak position, roughly corresponds to the space between the droplets elucidated from the microscopy observation. Figure 2 shows the time evolution of L_c during the isothermal phase separation at 38 °C. After the spinodal stage from 1 to 10 min, the time evolution of correlation lengths obeys the power law $L_c \sim t^{1/3}$, which is typical for the droplet growth caused by the hydrodynamic effect (Brownian coagulation)[12−14] or by the Lifshitz−Slyozov evaporation−concentration process.[15] Thus, we can find that the spinodal decomposition and subsequent coarsening processes similar to those for isotropic liquids and solids occur even in the liquid crystal system.[5,16] It should be noted that the power law $L_c \sim t^{1/3}$ has been observed when the growth of the nematic phase is restricted by increased confinement of the droplet boundary.[17]

When the sample was phase-separated for 60 min and then cooled to room temperature, the polymer-rich phase shrinks by

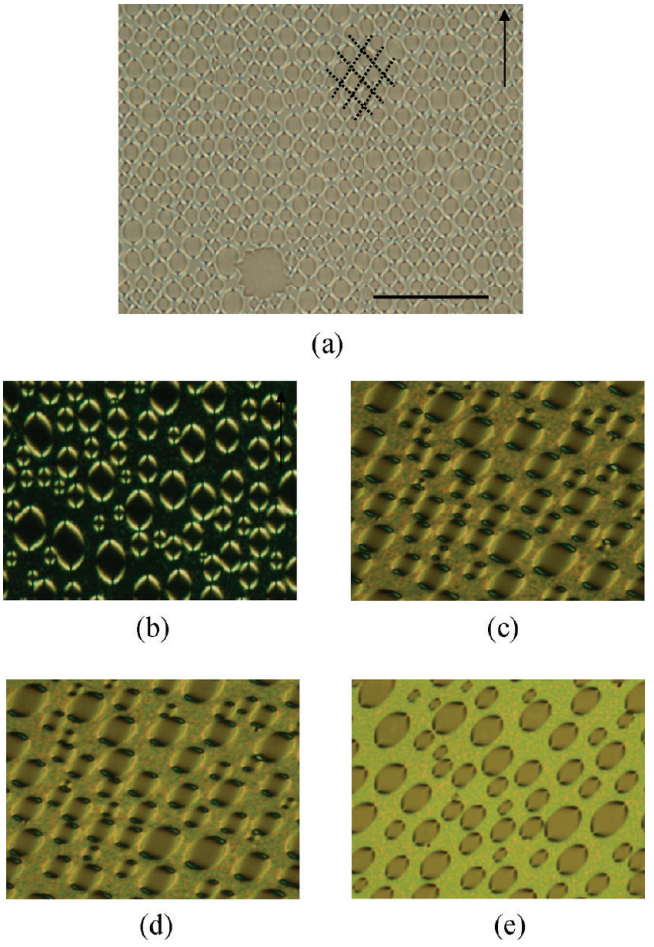

Figure 3. (a) Optical micrograph of the honeycomb network structure with a quasi-lattice (dashed lines), which is observed on cooling to room temperature at a rate of 0.5 °C/min after the isothermal phase separation for 60 min at 38 °C. Scale bar: 50 μm. (b−d) Polarized optical micrographs taken with different rotation angles of the sample stage: (b) 0°, (c) 15°, (d) 30°, and (e) 45°. The arrow in (a) and (b) indicates the rubbing direction.

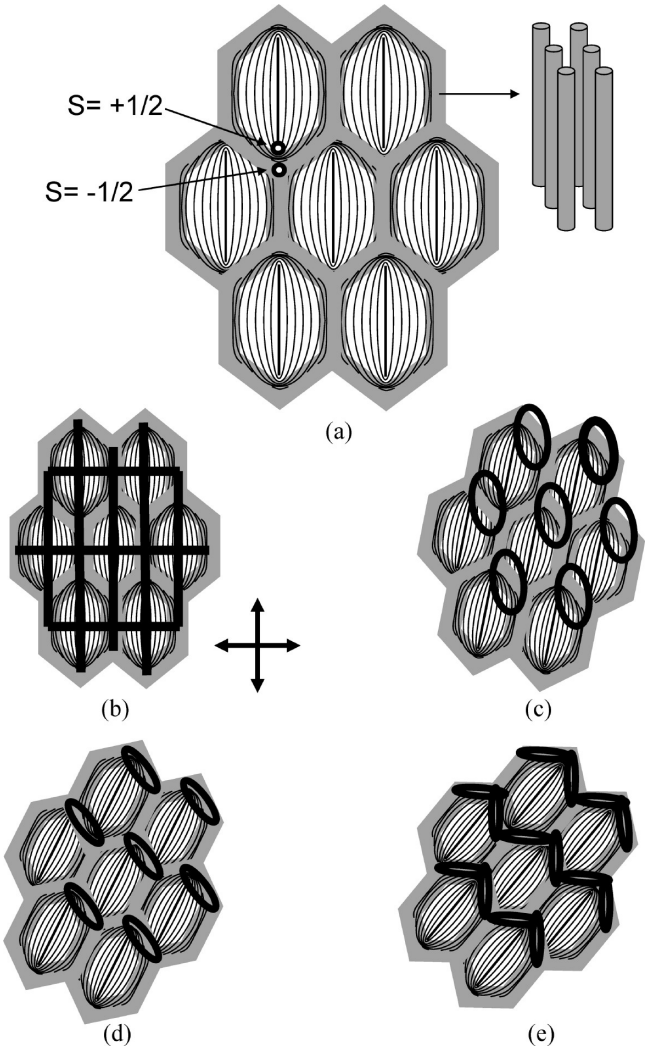

Figure 4. (a) Schematic illustration of molecular orientation in the honeycomb network segregation structure. (b−e) The expected brush curves observed with different rotation angles of the sample stage: (b) 0°, (c) 15°, (d) 30°, and (e) 45° (compare with Figures 3b−e).

expelling the LMW-LCM solvent into the LMW-LCM-rich droplets as expected from the phase diagram of Figure S1. As a result, excellent honeycomb network structure containing the LMW-LCM nematic phase within hollowlike microcells is formed as seen in the micrograph in Figure 3a. The average diameter of the hollowlike microcell is within 7−8 μm, 3 or 4 times larger than the width of the network wall. Since the thickness of sample cell is 3 μm, it can be said that the microcell is disklike. Note that such a honeycomb network remains unchanged over one month. Two reasons can be considered for the pinning phenomenon. One is due to the cylindrical microsegregation of the polystyrene block and the nematic−smectic transformation of the LC segment block in the LC-BP-rich phase since the LC-BP-rich phase increases its LC-BP weight fraction and then behaves like a pure LC-BP phase.[8] The resulting positional orders, like those in solid phases,[12] may significantly disrupt the coalescence of droplets as well as the diffusion of LMW-LCM from one droplet to another. The other is formation of a stable lattice of topological defects as mentioned below.

Of interest is that the shape of microcell is not circle, but ellipsoid. The long axis of the ellipsoid corresponds to the rubbing direction, i.e., the director of nematic LC. This anisotropic shape is due to the anisotropic alignment of LC in the microcell. POM texture shows characteristic orientation of LC molecules within the microcell. Figures 3b−e show the POM textures observed with cross-polarizers at different rotation angles of 0°, 15°, 30°, and 45°, respectively. The closed brush curves runs on the corner of network and show the characteristic patterns when the sample stage is rotated. Such closed brush curves are explained by the inversion wall with a pair of vertical $s = +1/2$ and $-1/2$ disclination lines joining the lower and upper surfaces of cell which have been created on the preceding nematic−nematic phase separation at 38 °C.[18,19] The $s = -1/2$ disclination line is located at the corner of the network wall, and the $s = +1/2$ line located in the microcell is near this corner, as shown in Figure 4a. The sign of these defects can be determined from the movement of the brushes caused by the rotation of the crossed polarizers (refer to Figures 4b−e).[18] The molecular arrangement of LMW-LCM within the microcell can be illustrated in Figure 4a; almost all the molecules are aligned along the rubbing direction, i.e., the orientation direction of initial monodomain nematic LC, although the directors are deformed near the corner to form the $s = +1/2$ disclination. In a network wall, the microcylinders of block copolymer lie parallel to the net as illustrated in the inset of Figure 4a. The thickness of the net is approximately 1−2 μm while the distance between microcylinders is about 20 nm. Thus, 50−100 microcylinders are included in the direction perpendicular to each net wall.

The anisotropic shape of ellipsoid resulting from the nematic−nematic phase separation is promoted by the distance d between

the two disclination lines of $s = +1/2$ and $s = -1/2$, which can be related to the surface anchoring energy W_s by the equation

$$d \sim (K/W_s)^{1/2} \quad (1)$$

where K is the Frank elastic constant.[19] The increase in W_s decreases d and hence increases the anisotropy of the ellipsoid in the LMW-LCM-rich microcell. On the other hand, the interfacial energy in the microdomain tends to decrease the shape anisotropy. Thus, the anisotropy of the ellipsoid domain is predominated by competition between surface anchoring energy and interfacial energy; the anisotropy is more distinct when the anchoring energy is larger than the interfacial energy.

Finally, note that such ellipsoid microcells align with some two-dimensional periodicity irrespective of the distribution of their sizes. In Figure 3a, the two-dimensional quasi-lattice is given by dashed lines; this is the reason why light scattering takes place in the limited directions that are tilted by 60° to the n-director. To our knowledge, no such periodic alignment of phase-separated droplets has been reported yet in the liquid−liquid system. Since in the nematic−nematic phase separation system the director field is connected through the two nematic phase domains, the elasticity of LC is also attributable to such a periodicity since the defects should be equally spaced over the nematic domain.[9,20,21]

In summary, we examined the LC-LC phase separation behavior from the homogeneously aligned monodomain nematic phase of the LMW-LCM/LC-BP (75/25) mixture system sandwiched between the rubbed substrates with a thickness of 3 μm. Droplets of the LMW-LCM-rich phase appear, and their size evolution follows the 1/3 power law expected for the growth of patterns caused by hydrodynamic interactions and the Lifshitz−Slyozov process found for isotropic liquid and solid mixtures. Because of the elasticity of LC, the droplets are well aligned with a two-dimensional quasi-lattice. When the sample cell is cooled to room temperature, the phase separation is almost pinned since the microcylindrical domain formation and nematic−smectic transformation of the LC-BP-rich phase disrupts further evolution of phase separation. Thus, we can obtain stable honeycomb network structure in which LMW-LCM phase is accommodated in a hollow microcell of approximately 7−8 μm diameter surrounded by a network wall of the LC-BP-rich phase with widths of 1−2 μm. In other words, a type of microcapsule spontaneously forms. The results presented in the study will provide insights into designing experiments on the control of LC domain morphologies in a LC polymer/LC mixture under nanoscopic confinement.

Acknowledgment. This research was supported by a Grant-in-Aid for Creative Scientific Research from the Ministry of Education, Science, Sports and Culture.

Supporting Information Available: Phase diagram of the LMW-LCM/LC-BP mixture system. This material is available free of charge via Internet at http://pubs.acs.org.

References and Notes

(1) Hashimoto, T. In *Material Science and Technology*; Thomas, E. L., Ed.; VHC: Weinheim, 1993; Vol. *12*, Chapter 6.
(2) *Polymer Alloys and Blends. Thermodynamics and Rheology*; Utracki, L. A., Ed.; Hanser: Munich, 1990.
(3) *Phase Transition Dynamics*; Onuki, A., Ed.; Cambridge University Press: Cambridge, 2002.
(4) *Liquid Crystals in Complex Geometries Formed by Polymer and Porous Networks*; Crawford, G. P., Zumer, S., Eds.; Taylor and Francis: London, 1996.
(5) Shiwaku, T.; Nakai, A.; Wang, W.; Hashimoto, T. *Macromolecules* **2005**, *38*, 10702.
(6) Ahn, W.; Ha, K.; Park, L. S. *Mol. Cryst. Liq. Cryst.* **2006**, *458*, 191.
(7) Tomikawa, N.; Lu, Z.; Itoh, T.; Imrie, C. T.; Adachi, M.; Tokita, M.; Watanabe, J. *Jpn. J. Appl. Phys.* **2005**, *44*, L711.
(8) Tokita, M.; Adachi, M.; Masuyama, S.; Takazawa, F.; Watanabe, J. *Macromolecules* **2007**, *40*, 7276.
(9) Xia, J.; Wang, J.; Lin, Z.; Qui, F.; Yang, Y. *Macromolecules* **2006**, *39*, 2247.
(10) Brown, G.; Chakrabarti, A. *J. Chem. Phys.* **1994**, *101*, 3310.
(11) Krausch, G.; Dia, C.; Kramer, E. J.; Marko, J. F.; Bates, F. S. *Macromolecules* **1993**, *26*, 5566.
(12) Binder, K.; Stauffer, D. *Phys. Rev. Lett.* **1974**, *33*, 1006.
(13) Furukawa, H. *Prog. Theor. Phys.* **1978**, *59*, 1072.
(14) Kawasaki, K.; Ohta, T. *Prog. Theor. Phys.* **1978**, *59*, 362.
(15) Lifshitz, I. M.; Slyozov, V. V. *J. Phys. Chem. Solids* **1961**, *19*, 35.
(16) Wang, W.; Shiwaku, T.; Hashimoto, T. *Macromolecules* **2003**, *36*, 8088.
(17) Chen, X.; Benjamin, D. H.; Shen, A. Q. *Langmuir* **2008**, *24*, 541.
(18) *Textures of Liquid Crystals*; Demus, D., Richter, L., Eds.; Verlag Chemie: Weinheim, 1979.
(19) Ryschenkow, G.; Kleman, M. *J. Chem. Phys.* **1976**, *64*, 404.
(20) Yamamoto, J.; Tanaka, H. *Nature* (*London*) **2001**, *409*, 321.
(21) Das, S. K.; Rey, A. D. *J. Chem. Phys.* **2004**, *121*, 9733.